Supplementary Information for

Phenotypic variation explains food web structural patterns

Jean P. Gibert, John P. DeLong

correspondence to: jeanphisth@gmail.com

This file includes:

Appendix A: A general framework to understand the effect of variation on predator intake rate and connectivity.

In this section we explain how to incorporate phenotypic variation into intake – or foraging – rates. We then show how phenotypic variation affects predator connectivity (i.e., the number of prey items, or diet breadth).

Let us assume that a predator eats a single prey item and the existence of a normally distributed trait with probability density function $p(x,\bar{x},\sigma^2)$, mean trait value $\bar{x}$ and variance σ^2 that controls their interaction. Previous work (1–4) has shown that the intake rate of the predator, assuming a type II functional response, can be written as:

$$f(R,C,x,\bar{x},X_{opt},\sigma^2)=\int_{-\infty}^{+\infty}\frac{\alpha(x,X_{opt})RC}{1+\alpha(x,X_{opt})\eta(x,X_{opt})R}p(x,\bar{x},\sigma^2)dx\,, \qquad [S1]$$

where R is the density of the prey and C is that of the predator. The function $\alpha(x,X_{opt})$ models how the attack rate of the predator changes with the underlying controlling trait x, which has empirically been observed to be maximal at an optimal trait value X_{opt} and to decay away from that value (e.g. (5)). In theoretical studies (e.g. (1, 3)), the function is typically assumed to be Gaussian:

$$\alpha(x)=\alpha_{\max}\exp\left[-\frac{\left(x-X_{opt}\right)^2}{2\tau^2}\right], \qquad [S2]$$

where τ is a shape parameter that controls how fast the attack rate decays away from the optimal trait value and $\alpha_{\max}$ is the maximal attack rate at $x = X_{opt}$. The function $\eta(x, X_{opt})$ models how the handling time of the predator changes with the underlying controlling trait, and has empirically been observed to be minimal at an optimal trait value X_{opt}, and to increase away form that value within a given predator species (e.g. (5)). Previous literature (e.g. (3, 4)) has typically modeled that relationship as:

$$\eta(x) = \eta_{\max} - \left(\eta_{\max} - \eta_{\min}\right)\exp\left[-\frac{\left(x-\theta_{\eta}\right)^2}{2\nu^2}\right], \qquad \text{[S3]}$$

where ν, as with τ, controls how steeply the handling time increases away from its minimal value at $x = X_{opt}$. Notice that the optimal value of the trait that maximizes the attack rate and minimizes the handling time needs not be the same for both parameters (3).

Under these assumptions, previous studies have shown that the intake rate changes with variation in the underlying trait, which has multiple consequences for predator-prey dynamics (1, 3, 4). Here, we extend this approach to a predator eating multiple prey types, as would be the case for a typical consumer within a food web. To do so, we note that the type II functional response has a simple extension from the single prey item case to multiple species of the form:

$$f_i(R_i, C) = \frac{\alpha_i R_i C}{1 + \sum_{j=1}^{n} \alpha_j \eta_j R_j}. \qquad \text{[S4]}$$

Equation [S4] specifies the intake rate of the predator with respect to its *i*-th prey, from a prey set composed of *n* species. Assuming that the attack rate and the handling time are, again, functions of a normally distributed trait we can average the intake rate across all possible trait values to get:

$$f_i(R_i, C, x, \bar{x}, X_{opt}, \sigma^2) = \int_{-\infty}^{+\infty} \frac{\alpha_i(x, X_{opt}) R_i C}{1 + \sum_{j=1}^{n} \alpha_j(x, X_{opt}) \eta_j(x, X_{opt}) R_j} p(x, \bar{x}, \sigma^2)\, dx \,. \qquad [S5]$$

For simplicity, we assume throughout the main text that X_{opt} is roughly the same for both the attack rate and the handling time, following empirical results (5), but this does not need to be the case (3). Equation [1] is controlled by two important parameters, phenotypic variation (σ^2) and phenotypic mismatch ($d^2 = \left(X_{opt} - \bar{x}\right)^2$), or the difference between the optimal trait value and the mean trait value in the population. The phenotypic mismatch is then a proxy for maladaptation, or predator specialization on a given prey. Because of the many factors controlling maladaptation, a predator will presumably have differing levels of maladaptation among its many prey items (6, 7). We thus assume a different d^2 for each prey item, which allows us to assess how different levels of variation in the underlying trait will affect the intake of the predator for each prey item prey item (Fig. 1, main text). In the main text we only explored one possible combination of parameters ($\tau = \nu = 1$ and the trait optimum X_{opt} being the same for both the attack rate and the handling time). Here, we show that the results in the main text also hold for different values of the parameters τ and ν (Fig S1). We also show that our results hold for a situation in which the optimum trait value is different for the attack rate and the handling time (Fig S2).

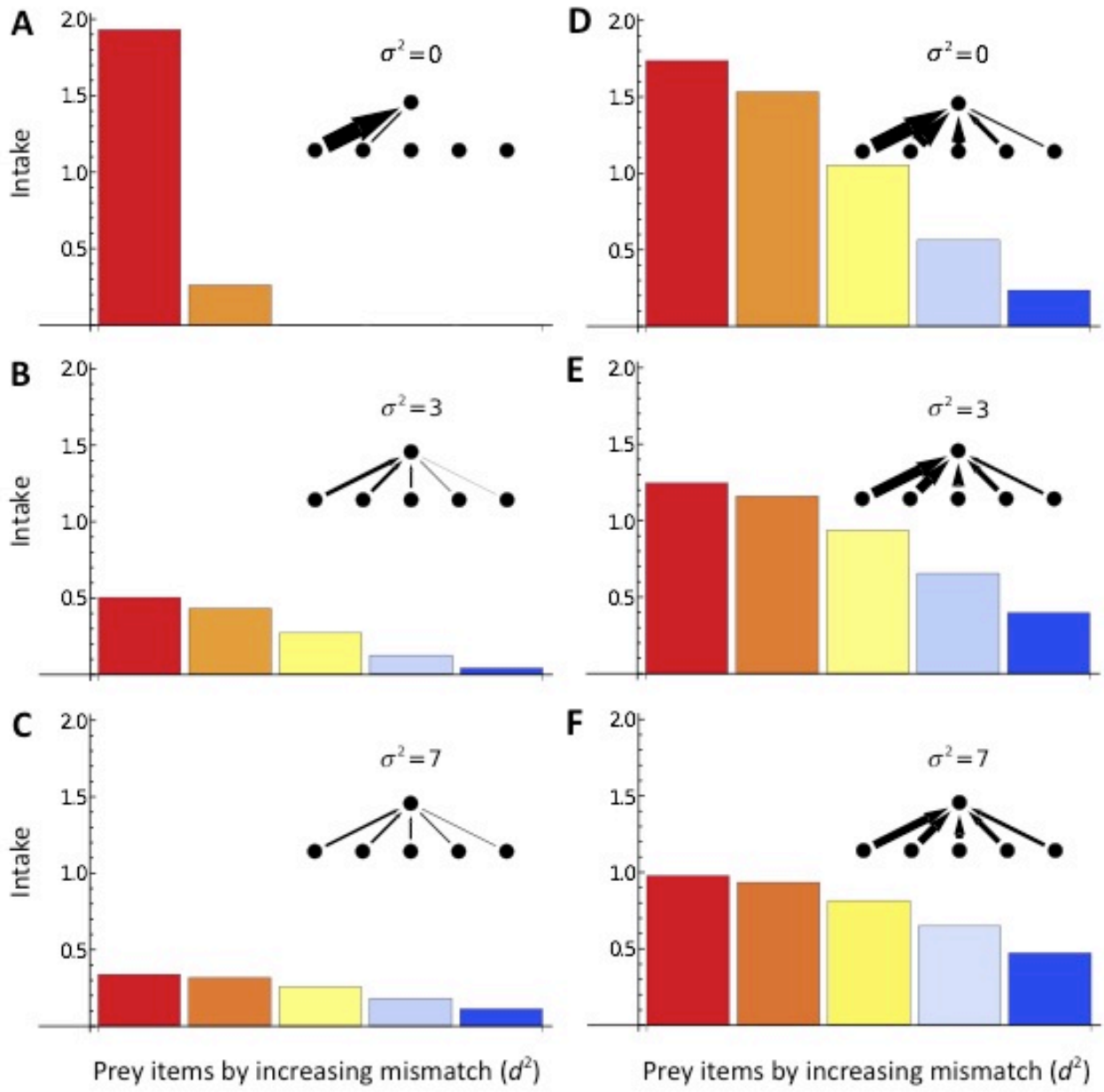

Fig S1: **A-C**, same as in Fig 1 of the main text, but for $\tau = \nu = 0.5$. **D-F**, same as in **A-C** but for $\tau = \nu = 2$. In both cases it can be seen that both the number and the strength of the connections is affected by an increase in variation. The effect in the number is stronger for lower values of the parameters (**A-C**) than for larger values (**D-F**), while the total intake seems to be overall larger when for larger values of the parameters (**D-F**).

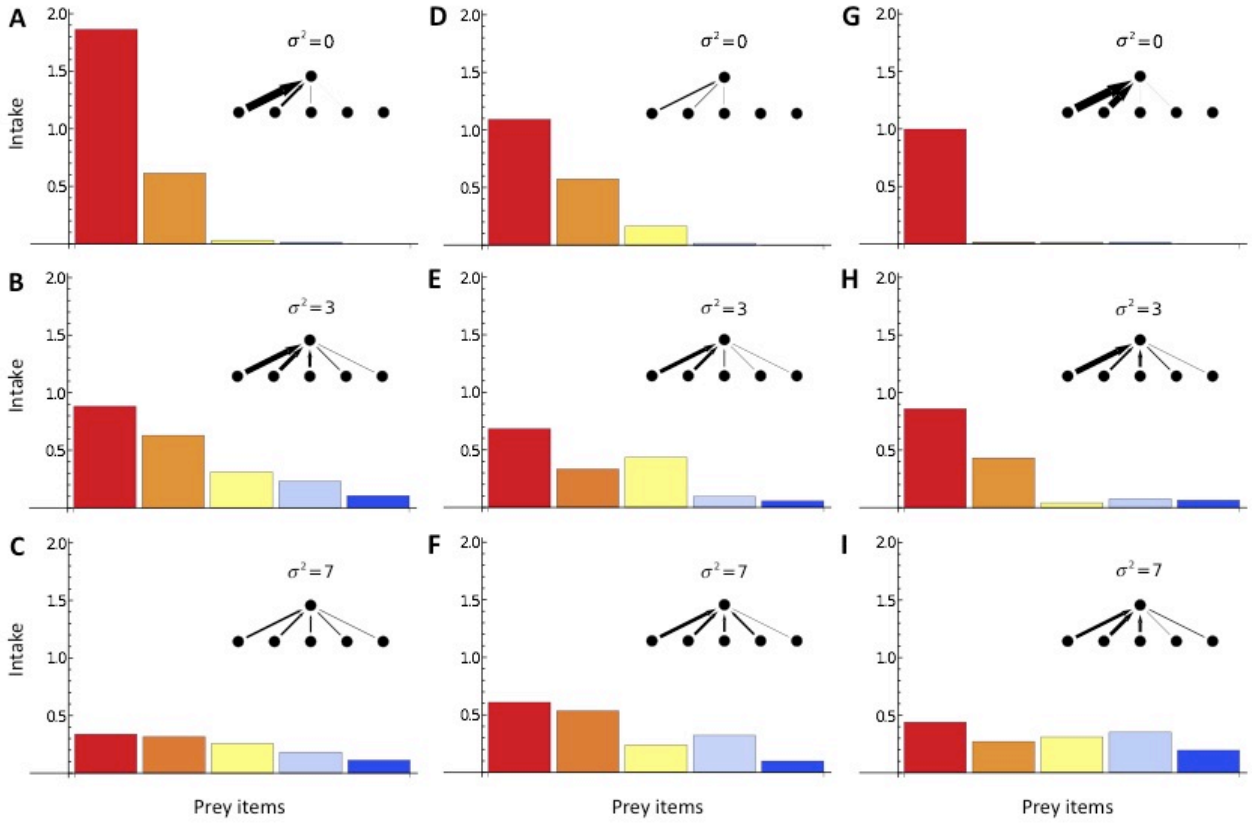

Fig S2: To assess a potential effect of having different X_{opt} for the attack rate and the handling time, we added different random value sampled from the closed interval [0, $X_{\max}$] for each prey item and level of variation, then added that value to X_{opt} only for the attack rate. We did that for three different values of $X_{\max}$ (**A-C**, $X_{\max}=1$; **D-F**, $X_{\max}=2$; **G-I**, $X_{\max}=3$). It can be seen that at larger levels of $X_{\max}$, the intake rate of the predator has greater levels of randomness, as expected, but the overall effect of variation on the number and strength of interactions –that increasing variation leads to a larger number of weaker interactions– remains unchanged.

Appendix B: Total intake rate among all prey items.

In this section we show how to find the total intake rate for a given predator and how that quantity changes with phenotypic variation, as shown in Fig 2 of the main text. Building upon equation [S5], the total intake rate for a given predator preying upon *n* species is:

$$f_{tot}(R_i, C, x, \bar{x}, X_{opt}, \sigma^2) = \sum_{i=1}^{n} \int_{-\infty}^{+\infty} \frac{\alpha_i(x, X_{opt}) R_i C}{1 + \sum_{j=1}^{n} \alpha_j(x, X_{opt}) \eta_j(x, X_{opt}) R_j} p(x, \bar{x}, \sigma^2) dx \,. \quad [S6]$$

It is possible to obtain some intuition as to how [S6] behaves analytically. First, let us assume that the handling time is zero, so that we are effectively dealing with a type I functional response. In such a scenario, [S6] reduces to:

$$f_{tot}(R_i, C, x, \bar{x}, X_{opt}, \sigma^2) = C \sum_{i=1}^{n} R_i \int_{-\infty}^{+\infty} \alpha_i(x, X_{opt}) \, p(x, \bar{x}, \sigma^2) dx \,. \quad [S7]$$

Through integration we get:

$$f_{tot}(R_i, C, \bar{x}, X_{opt}, \sigma^2) = C \sum_{i=1}^{n} R_i \frac{\alpha_{\max} \tau}{\sqrt{\tau^2 + \sigma^2}} \exp\left[-\frac{1}{2} \frac{d^2}{\tau^2 + \sigma^2} \right]. \quad [S8]$$

We now notice that for large enough σ^2, $1/x^2$ is larger than $\exp(-x)$, which implies:

$$\frac{2\left(\tau^2 + \sigma^2\right)}{x^2} > \exp\left(-\frac{1}{2} \frac{x}{\tau^2 + \sigma^2} \right), \quad [S9]$$

for large enough *x*. Assuming that d^2 increases by one with each prey item, and thus assuming the existence of a prey item for which the mismatch is small or null and an increasing mismatch for all other species, we can write [S8] as,

$$f_{tot}(R_i, C, \bar{x}, X_{opt}, \sigma^2) = C\sum_{i=1}^{n} R_i \frac{\alpha_{\max}\tau}{\sqrt{\tau^2+\sigma^2}} \exp\left[-\frac{1}{2}\frac{i^2}{\tau^2+\sigma^2}\right]. \quad [S10]$$

Using [S8] and [S10] we obtain,

$$f_{tot}(R_i, C, \bar{x}, X_{opt}, \sigma^2) = C\sum_{i=1}^{n} R_i \frac{\alpha_{\max}\tau}{\sqrt{\tau^2+\sigma^2}} \exp\left[-\frac{1}{2}\frac{i}{\tau^2+\sigma^2}\right] < C\sum_{i=1}^{n} R_i \frac{\alpha_{\max}\tau}{\sqrt{\tau^2+\sigma^2}} 2(\tau^2+\sigma^2)\frac{1}{i^2}. \quad [S11]$$

Assuming Ri=C=1, for simplicity (we are just interested in the effect of σ^2, not on the effect of density), we can rearrange [S11] into,

$$f_{tot}(R_i, C, \bar{x}, X_{opt}, \sigma^2) < 2\alpha_{\max}\tau\sqrt{\tau^2+\sigma^2}\sum_{i=1}^{n}\frac{1}{i^2}, \quad [S12]$$

which, using the fact that $\sum_{i=1}^{+\infty}\frac{1}{i^2}$ converges to $\pi^2/6$, yields:

$$f_{tot}(R_i, C, \bar{x}, X_{opt}, \sigma^2) < \frac{1}{3}\alpha_{\max}\tau\pi^2\sqrt{\tau^2+\sigma^2}. \quad [S13]$$

Equation [S13] shows that, at most, the total intake rate grows as the square root of the phenotypic variation (Fig S3). In the main text we showed that increasing variation increased the total intake rate (Fig 2), but while doing so, we assumed that handling time was independent from phenotypic variation. Here we show that the results in the main text hold when the handling time changes with phenotypic variation as well (Fig S4-**A**). We also show that our results hold for larger sets of prey items (Fig S4-**B**), and for changes in phenotypic mismatch from one prey species to the next that are smaller, and hence, more conservative (Fig S4-**C**).

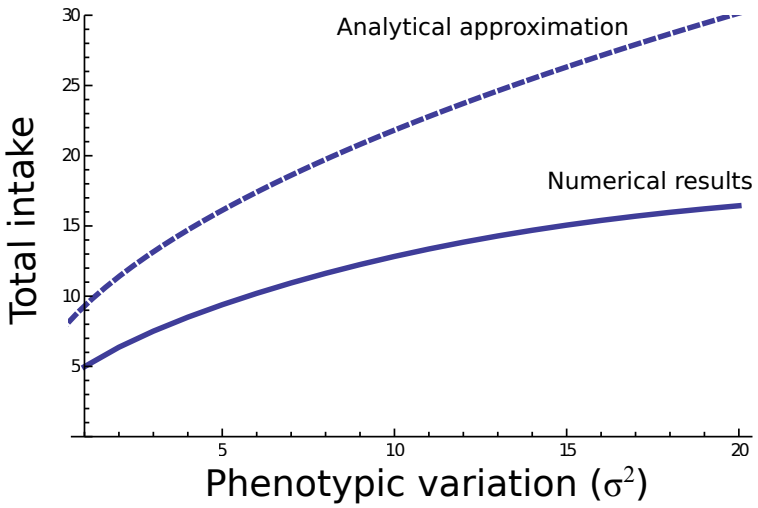

Fig S3: Dashed, plot of the predicted increase in total intake rate with phenotypic variation for a very large set of species as predicted analytically (dashed), and as found numerically (solid). Notice that while our numerical approximation suggests an increase of the total intake rate that goes as the square root of the phenotypic variation, our numerical results show a slightly lower increase, as expected, but an increase nonetheless.

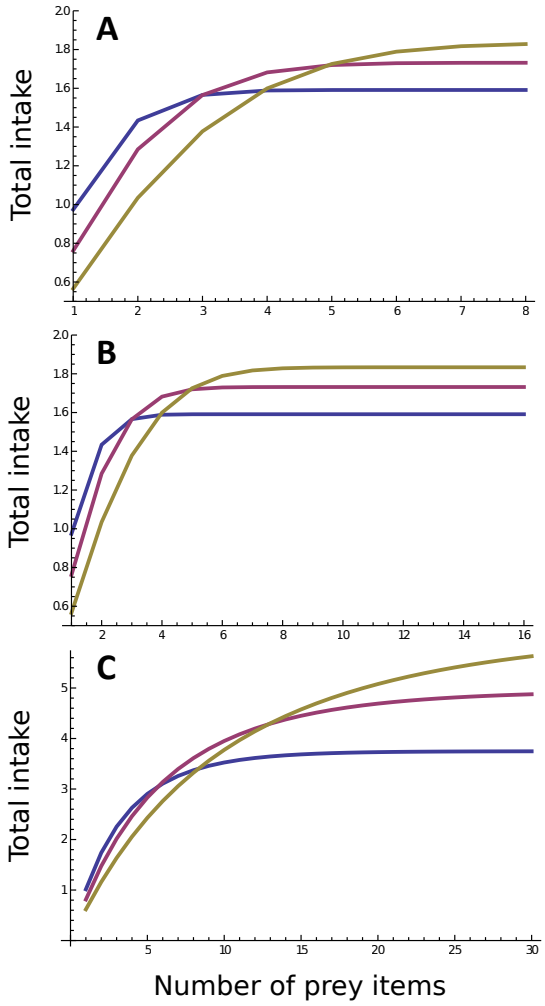

Fig S4: **A.** Plot of an increase in the total intake rate assuming a change in both the attack rate and the handling time for 8 species and all parameters as in the main text and previous appendices. **B.** Same as in **A** but for a larger set of species (16 species). **C.** Intake rate as a function of an even number set of species, where the phenotypic mismatch (d^2) increases by one for each additional prey item rather than as the square of the prey item's index, as assumed in the main text. It can be seen that results are qualitatively the same, only that the place where curves cross moves to the right.

Appendix C: Phenotypic variation and trophic level.

In this section we show how to assess the effect of phenotypic variation on the trophic level of the focal predator. As explained in the main text, the trophic level of a species in a food web is given by:

$$TL_j = 1 + \sum_{i=1}^{N} p_{ij} TL_i \,, \qquad \text{[S14]}$$

where, TLi is the trophic level of prey i, and pij is the fraction of the diet of species j that species i constitutes (8). We notice that pij can be written as:

$$p_{ij} = \frac{f_i(R_i, C_j, x, X_{opt})}{\sum_{k=1}^{N} f_k(R_k, C_j, x, X_{opt})} \,, \qquad \text{[S15]}$$

this is, the intake rate of species j when consuming species i divided by the sum of the intake rates from all species consumed. Then, as explained in the main text, *TLj* can be expressed as:

$$TL_j = 1 + \sum_{i=1}^{N} \frac{f_i(R_i, C_j, x, X_{opt})}{\sum_{k=1}^{N} f_k(R_k, C_j, x, X_{opt})} TL_i \,. \qquad \text{[S16]}$$

After averaging *TLj* over the probability density function of the trait we get:

$$TL_j = 1 + \sum_{i=1}^{N} TL_i \int_{-\infty}^{+\infty} \frac{f_i(R_i, C_j, x, X_{opt})}{\sum_{k=1}^{N} f_k(R_k, C_j, x, X_{opt})} p(x, \bar{x}, \sigma^2) dx \,, \qquad \text{[S17]}$$

as explained in the main text. Using [S17], we can keep track of how the trophic level of a predator changes as predator-prey dynamics unfold for a given predator-prey model.

To assess how this change may occur, we can use a three-species predator-prey model with a basal resource, an intermediate consumer that preys upon the basal resource, and an omnivorous top predator that preys upon both the consumer and the basal resource. Such a model can take the form,

$$\frac{dR}{dt} = rR\left(1 - \frac{R}{K}\right) - \frac{\alpha_C RC}{1 + \alpha_C \eta_C R} - \frac{\alpha_{RT} RT}{1 + \alpha_{RT} \eta_{RT} R}$$

$$\frac{dC}{dt} = \varepsilon_C \frac{\alpha_C RC}{1 + \alpha_C \eta_C R} - \frac{\alpha_{CT} CT}{1 + \alpha_{CT} \eta_{CT} C} - d_C C\,, \qquad \text{[S18]}$$

$$\frac{dT}{dt} = \varepsilon_{RT} \frac{\alpha_{RT} RT}{1 + \alpha_{RT} \eta_{RT} R} + \varepsilon_{CT} \frac{\alpha_{CT} CT}{1 + \alpha_{CT} \eta_{CT} C} - d_T T$$

where equations keeps track of the rate of change of the basal resource (R), the intermediate consumer (C) and the top omnivore consumer (T) over time, r is the per-capita or maximum growth rate of the resource, K is the carrying capacity of the resource, ε parameters stipulate the rate at which prey individuals are converted into predators and d parameters are the death rate of consumers, with all other parameters as before. For a given parameter combination, we can see how the trophic level of the top consumer, as defined in equation [S16], is now a dynamical quantity that changes over time as the ecological dynamics in [S18] unfold (Fig S5).

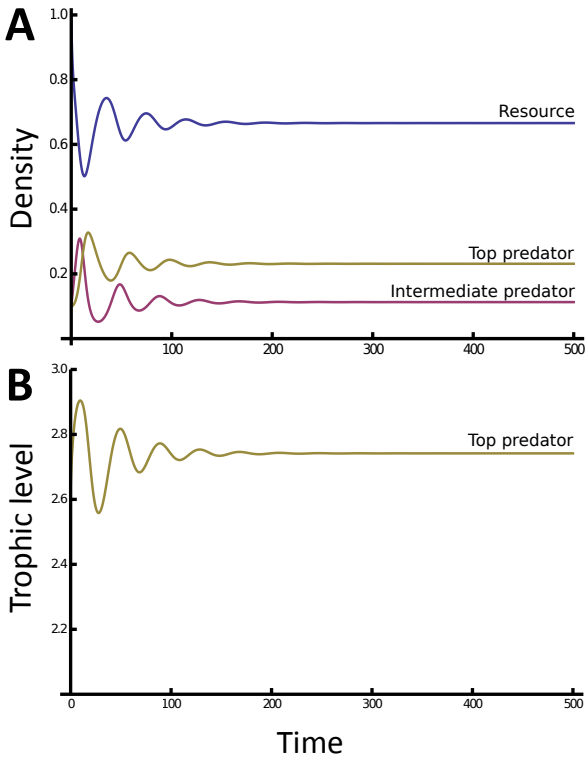

Fig S5: **A**. Population dynamics for the system in [S18] with parameters as before. **B**. Plot of the trophic level of the top predator and its change over time as ecological dynamics unfold. We can see that as the density of both prey items change over time, so does how much the top predator relies on either one of them, which leads to fluctuations in its trophic level.

To assess how phenotypic variation determines the trophic level of the focal predator, we can, following previous literature (1, 3, 4) and rewriting the system in [S18] as a function of an underlying trait controlling the interaction between the top predator and its prey as:

$$\frac{dR}{dt} = rR\left(1-\frac{R}{K}\right) - \frac{\alpha_C RC}{1+\alpha_C \eta_C R} - \int_{-\infty}^{+\infty} \frac{\alpha_{RT} RT}{1+\alpha_{RT}\eta_{RT} R}\, p(x,\bar{x},\sigma^2)\, dx$$

$$\frac{dC}{dt} = \varepsilon_C \frac{\alpha_C R C}{1+\alpha_C \eta_C R} - \int_{-\infty}^{+\infty} \frac{\alpha_{CT} C T}{1+\alpha_{CT}\eta_{CT} C} p(x,\bar{x},\sigma^2)\,dx - d_C C\,, \qquad [S19]$$

$$\frac{dT}{dt} = \int_{-\infty}^{+\infty} \left(\varepsilon_{RT} \frac{\alpha_{RT} R T}{1+\alpha_{RT}\eta_{RT} R} + \varepsilon_{CT} \frac{\alpha_{CT} C T}{1+\alpha_{CT}\eta_{CT} C} \right) p(x,\bar{x},\sigma^2)\,dx - d_T T$$

where the attack rates and the handling times of the top predator are functions of the underlying trait as assumed in equations [S2] and [S3]. We can then use equation [S17] to keep track of how the trophic level of the focal predator changes with a change in the phenotypic variation, σ^2. To produce Fig 3c, d of the main text, we ran the above model for increasing levels of σ^2, then extracted the trophic level of the top predator using [S17] after the system reached equilibrium (after a 100 time steps), and plotted the extracted equilibrium trophic levels against σ^2 for a given combination of parameters (we assumed handling time was independent of variation, as making this further assumption does not qualitatively affect our results; see Appendices A and B). Parameter values were chosen to ensure the persistence of the three species: $r = K = \alpha_C = \alpha_{RT} = \alpha_{CT} = \tau = 1$, $\varepsilon_C = 0.5$, $\varepsilon_{RT} = 0.04$, $\varepsilon_{CT} = 0.64$, the maximal handling times for both predators were 0.04, both consumers' death rates (*d*) were 0.1, and the phenotypic mismatch of the top predator with the basal resource was 0 and 4 with the intermediate consumer in Fig 3c, and the other way around in Fig 3d.

To assess how trophic level and predator connectivity (or diet breath) change together with phenotypic variation (Fig 3e, f), we made some simplifying assumptions. First, we noticed that the system in [S19] can be seen as a simplified version of a more complex scenario where instead of having one basal resource and one intermediate consumer, there are *n* basal resources and *m* intermediate consumers. The equations controlling the dynamics of such as system are:

$$\frac{dR_i}{dt} = rR_i\left(1-\frac{R_i}{K}\right) - \sum_{j=1}^{m}\frac{\alpha_{R_iC_j}R_iC_j}{1+\sum_{k=1}^{n}\alpha_{R_kC_j}\eta_{R_kC_j}R_k} - \int_{-\infty}^{+\infty}\frac{\alpha_{R_iT}R_iT}{1+\sum_{k=1}^{m}\alpha_{R_kT}\eta_{R_kT}R_k+\sum_{k=1}^{n}\alpha_{C_kT}\eta_{C_kT}C_k}p(x,\bar{x},\sigma^2)\,dx$$

$$\frac{dC_j}{dt} = \sum_{i=1}^{n}\frac{\varepsilon_{R_iC_j}\alpha_{R_iC_j}R_iC_j}{1+\sum_{k=1}^{n}\alpha_{R_kC_j}\eta_{R_kC_j}R_k} - \int_{-\infty}^{+\infty}\frac{\alpha_{C_jT}C_jT}{1+\sum_{k=1}^{n}\alpha_{C_kT}\eta_{C_kT}C_k}p(x,\bar{x},\sigma^2)\,dx - d_{C_j}C_j \quad , \qquad \text{[S20]}$$

$$\frac{dT}{dt} = \int_{-\infty}^{+\infty}\left(\sum_{i=1}^{n}\frac{\varepsilon_{R_iT}\alpha_{R_iT}R_iT}{1+\sum_{k=1}^{n}\alpha_{R_kT}\eta_{R_kT}R_k}+\sum_{j=i}^{m}\frac{\varepsilon_{C_jT}\alpha_{C_jT}C_jT}{1+\sum_{k=1}^{m}\alpha_{C_kT}\eta_{C_kT}C_k}\right)p(x,\bar{x},\sigma^2)\,dx - d_TT$$

with all parameters as before. The system in [S19] is very hard to solve numerically, let alone analytically, so we can reduce the complexity of the problem by assuming that all species have similar parameters (ecological equivalency), and 1) that the attack rate for all intermediate consumers with the basal resource is $\alpha_{RC} = \beta / m$, that of the top predator with all intermediate consumers is $\alpha_{CT} = \nu / m$, and that of the top predator with all basal resources is $\alpha_{RT} = \gamma / m$, with parameters β, ν, γ being constant. Assuming low handling times, the system in [S20] can be approximately described by [S19], if we note that C and R in [S19] will now be keeping track of the change in the sum of all basal resource densities on the one hand, and the sum of all intermediate consumer densities in the other hand. We note that when it comes down to the trophic level of the top predator, having more intermediate consumers or basal resources only makes the tropic level of the top predator become closer to 2 (in case of having more basal resources) or closer to 3 (in case of having more intermediate consumers), but should not qualitatively affect how variation for the top predator affects its trophic level. In the main text, we thus assume that all species are equivalent to understand how phenotypic variation jointly affects

trophic level and connectivity, which greatly simplifies solving [S20] numerically, as we can use the much simpler [S19] instead.

So, to generate Fig 3e, f we assumed the top predator had access to at most 20 resources (either basal or intermediate), and then did as explained in Appendix A and counted the number of non-zero intake rates the predator could have among that potential set of prey for levels of phenotypic variation varying between 0 and 10, with a step of 0.2. We concomitantly ran [S19] in the same way described before (with parameter values as in all other appendices), and extracted the trophic level for the top predator for variation between 0 and 10 and the same step size. For Fig 3e, the predator had a smaller mismatch with the basal resource (d^2=0) and a larger mismatch with the intermediate consumer (d^2=2), while the opposite was true for Fig 3f. Our approach is thus assuming 1) all species are equal, 2) that regardless of how many connections the top predator can have, the strength of those connections is in one case larger with basal species than with intermediate ones (Fig 3e, because of smaller mismatch), and in one case larger with intermediate consumers than with basal resources (Fig 3f, again, because of the smaller mismatch with these species). Because of these assumptions, our theoretical predictions necessarily are qualitative, not quantitative, and we simply cannot make quantitative predictions for any given food web as of now.

Alternatively, we can use an approach similar to that used in Appendix A: we assume all species have different levels of mismatch, we assume that the system is at some sort of equilibrium where all prey species have similar densities roughly equal to 1, and then we simply use [S17] in the same way equation [S5] was used to find the number of connections. To do so, we specify the number of basal resources and consumers eaten by the top predator (10 and 10 to match what we did for the total connectivity, but different numbers are possible), we then specify

the levels of phenotypic mismatch as $d_i^2 = \phi + i - 1$ for basal resources, and $d_j^2 = \psi + i - 1$ for consumers (as per Appendix A). In this way we can still assess what happens when predators are generally better at eating basal resources vs eating intermediate resources based on their mismatch. Notice that in so doing, we give the predator a slight edge at eating species at one level or the other, but this does not mean that it is better of eating all species at one level rather than the other. For example: assume ϕ = 0 and ψ =2, the mismatch with the 1st and 2nd basal resources is smaller or equal to the 4th and 5th intermediate consumers, which is totally controlled by the numbers chosen. Our results hold in this case, with an increasing relation between trophic level and connectivity when the mismatch of the predator is smaller with basal resources (Fig S6 **A**), and the opposite being true when the mismatch of the top predator is smaller with intermediate consumers (Fig S6 **B**).

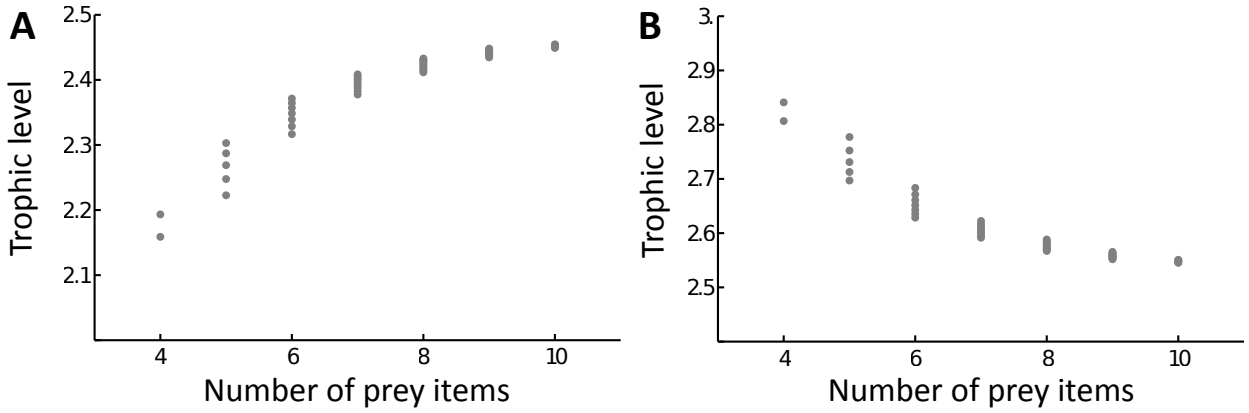

Fig S6: Trophic level against predator connectivity (**A**. $d^2 = 0$ with basal resources, $d^2 = 2$ with intermediate consumers, **B**. $d^2 = 0$ with intermediate consumers, $d^2 = 2$ with basal resources).

Appendix D: Interaction strengths.

Here, we show how we standardized interaction strengths across food webs to produce Fig. 5 of the main text. Only a subset of all analyzed food webs were quantitative, meaning that there was information on interaction strengths, or proxies of interaction strengths, only for 18 out of 58 food webs. These measures of interaction strengths were collected by the original researchers that compiled each food web, and this was done independently in each study (Table S1, Appendix E). As a consequence, the way interaction strengths were measured varies across all analyzed food webs but is consistent within food webs.

To test our prediction from Fig. 3g, h, of the main text, we regressed the interaction strength of all predators against the trophic level of all their prey, within each food web, and for all quantitative food webs. Because of this, the different measures of interaction strength across only need to be consistent within each food web, not across food webs, so a standardization procedure was not needed to test our prediction. However, we chose to standardize all measures of interaction strengths across food webs to make it easier for readers to follow Fig. 5 of the main text, where all plots were presented with the y-axis in the same units, as opposed to a figure where each plot had a slightly different measure of interaction strength.

Because measures of interaction strengths varied in the data used from direct quantifications of energy flow between species (e.g. in mg of C/m^2) to the number of instances a given predator-prey interaction was observed, to the relative importance a given prey played in a predator diet (either in proportion or percentage, see Table S1 in Appendix E), we chose to standardize them all by rescaling them into a number between 0 and 1. To do so, we divided each measure of interaction strength for a given predator and prey, by the sum of all interaction strengths for that predator across all its prey items. The result is a number between 0 and 1, that can be interpreted as a measure of the impact each prey has on their predators, relative to the

impact of all the other prey of that predator. For food webs where interaction strengths were already given as relative proportion of a given prey in a predator's diet, we simply used that as our proxy of interaction strength.

We notice that while experimentally, there is a long tradition of measuring interaction strengths as the difference in prey abundance before and after removal of a given predator (e.g. (9)), in which case interaction strengths can be either positive or negative, such measurements are rarely ever provided for entire food webs, as it would be immensely time consuming to do species removals, and probably unfeasible, for many of them. For entire food webs, measurements of interaction strengths typically are direct quantifications of energy flux or the positive effect of a given prey has on a predator, quantified as the number of times the predator-prey interaction was observed in the field, or similar means (e.g. (10–13)). As a consequence, our food webs do not have any negative interaction strengths –or the negative impact of predators on preys– and our measures of interaction strengths therefore need to be interpreted as the effect prey have on predators through the transference of energy and mass that is a consequence of predation. However, our theoretical approach predicts an expected relationship between the interaction strength, quantified as the effect of the prey on the predator (i.e. through intake rates), and the trophic level of said prey. In other words, the data we have is actually very well suited to test the predictions in Fig 3.

Last, because food webs are bottom-heavy (there are more species at lower trophic levels than at higher trophic levels) it is conceivable, in principle, that our ability to quantify interaction strengths, and their naturally occurring variation, would be worse at higher trophic levels than at lower trophic levels, just because there are fewer species at higher trophic levels. While this is a remote possibility, we nevertheless used a bootstrapping procedure that aims at minimizing the potential bias that food web structure would introduce in our analysis (i.e. the disproportionately

large effects of error in interaction strength quantification at higher trophic levels). To do this, we put together a table for each food web, with the observed standardized interaction strength between each predator-prey pair, and the trophic level of the prey, for all preys and predators. Then, we resampled each of such datasets 200 times with replacement, to regress, each time, the interaction strength of predators and their prey against the trophic level of each of their prey, for each food web separately. Each resampled dataset has a lower chance of having data from predator-prey interactions with prey from higher trophic levels, just because there are fewer of them, resulting in a lower chance of resampling these data. This, in turn, diminishes the impact of these rarer data points on the regression.

It can be seen that the results in Fig 5 of the main text are quite robust (Fig S7), and that most food webs actually show a negative relationship between interaction strength and the trophic level of prey, meaning that predators seem to relay less and less on prey from upper trophic levels.

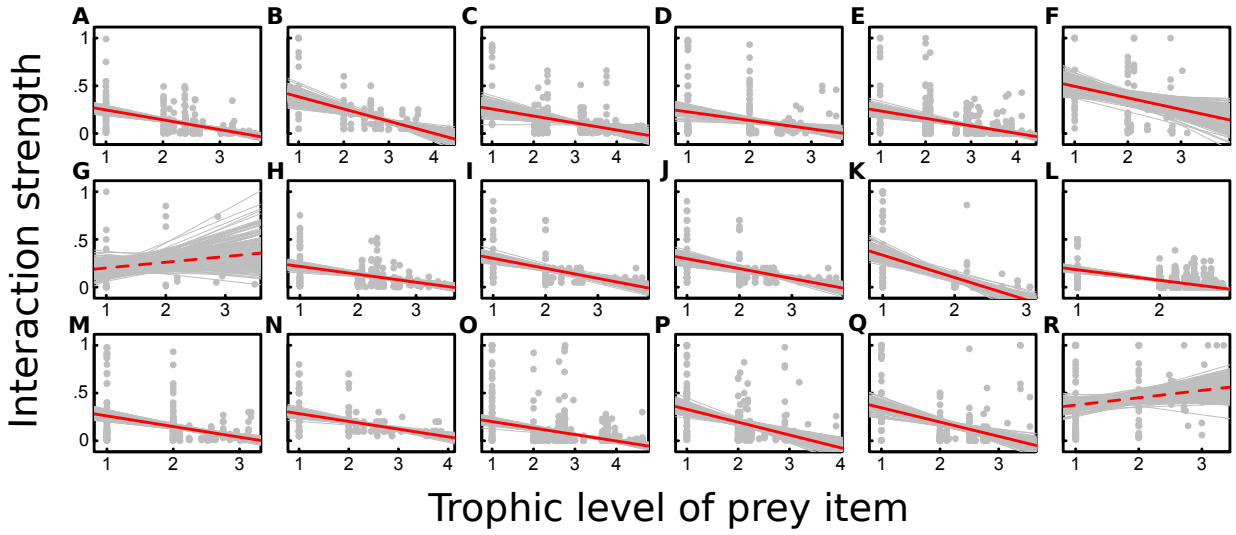

Fig S7: Grey dots represent a specific predator-prey pair within each food web, grey lines are bootstrap regressions (one per bootstrap replicate), and red lines represent a simple linear

regression, as in the main text. Each panel as in the main text: (a) Alvarado, (b) Angola, (c) Braço Morto, (d) Cádiz, (e) Chesapeake, (f) Corrente, (g) Huizache, (h) Itaipú (83-87), (i) Itaipú (88-92), (j) Mondego, (k) Northern California, (l) Onca, (m) Paraná, (n) Reef, (o) Scotia Sea, (p) St. Marks, (q) St. Martin, (r) UK Grassland.

Appendix E: Food web data

Fig. 4 food webs: from left to right and from top to bottom are: Skipwidth, St Marks, St Martin, Coachella Valley, Chesapeake, UK Grassland, Bridge Brook, Carpintería, Troy, Martins, Herlzler, Cooper, Venlaw, Berwick, North Col, Powder, Kye Burn, Sutton Autumn, Sutton Spring, Sutton Summer, Healy Creek, Dempsters Autumn, Dempsters Spring, Dempsters Summer, Stony Stream, Canton Creek, Black Road Stream, Broad Stream, Saguaro, Monterey Bay, Pawnee, Mojave parasitoids, Osa scavengers, Deep Creek, Aire, Paraná, Itaipú (83-87), Itaipú (88-92), Corrente, Angola, Braço Morto, Onca, Mondego, Vilas, Antarctica, Huizache, Alvarado, Quick Pond, Northern California, Las Cuevas, Cádiz ,Scotia Sea, Bear, Wet tropics, Porteirinho, Sarracenia, Benguela, Coral Reef.

Table S1: All food webs used, with some summary descriptors (S=number of species, L=number of connections or links, C=directed connectance of the food web, calculated as L/S^2, whether the food web is quantitative (Y/N), and the units of that measure (percent or proportion of total ingestion by a given predator, the frequency of predation events witnessed, energy flux)), the country of provenance, continent, ecosystem, type of food web and original reference.

FW name	Country	Continent	Ecosystem	Type	S	L	C	Quantitative (Y/N) and Original Units	Reference
Benguela	South Africa	Africa	Marine	Aquatic	29	203	0.24	N	Yodzis 1998
Skipwidth	UK	Europe	Pond	Aquatic	37	380	0.28	N	Warren 1989
St Marks	US	North America	Estuary	Aquatic	48	221	0.10	Y, Percent of diet	Christian & Luczkovich 1999
St Martin	France/St. Maarten	Caribean/Antilles	Island	Terrestrial	44	218	0.11	Y, Frequency of predation events	Goldwasser & Roughgarden 1993
Coral Reef	US/UK	Caribean/Antilles	Marine	Aquatic	50	556	0.22	Y, Proportion of diet	Opitz 1996
Coachella Valley	US	North America	Desert	Terrestrial	30	290	0.32	N	Polis 1991
Chesapeake	US	North America	Estuary	Aquatic	33	72	0.07	Y, Energy flux (mg/m^2 of carbon)	Baird & Ulanowicz 1989
UK Grassland	UK	Europe	Grassland	Terrestrial	87	126	0.02	Y, Frequency of predation events	Martinez et al 1999
Bridge Brook	US	North America	Lake	Aquatic	75	543	0.10	N	Havens 1992
Carpintería	US	North America	Marsh	Wetland	128	2290	0.14	N	Lafferty et al 2006
Troy	US	North America	Stream	Aquatic	76	177	0.03	N	Jarsma et al 1998
Martins	US	North America	Stream	Aquatic	104	342	0.03	N	Thompson & Townsend 2003
Herlzler (Coweeta 17)	US	North America	Stream	Aquatic	71	148	0.03	N	Thompson & Townsend 2003

Cooper (Coweeta 1)	US	North America	Stream	Aquatic	58	126	0.04	N	Thompson & Townsend 2003
Venlaw	New Zealand	Oceania	Stream	Aquatic	65	185	0.04	N	Thompson & Townsend 2003
Berwick	New Zealand	Oceania	Stream	Aquatic	77	240	0.04	N	Thompson & Townsend 2003
North Col	New Zealand	Oceania	Stream	Aquatic	78	241	0.04	N	Thompson & Townsend 2003
Powder	New Zealand	Oceania	Stream	Aquatic	78	268	0.04	N	Thompson & Townsend 2003
Kye Burn	New Zealand	Oceania	Stream	Aquatic	98	629	0.07	N	Thompson & Townsend 2003
Sutton Autumn	New Zealand	Oceania	Stream	Aquatic	80	335	0.05	N	Thompson & Townsend 2003
Sutton Spring	New Zealand	Oceania	Stream	Aquatic	74	391	0.07	N	Thompson & Townsend 2003
Sutton Summer	New Zealand	Oceania	Stream	Aquatic	86	423	0.06	N	Thompson & Townsend 2003
Healy Creek	New Zealand	Oceania	Stream	Aquatic	96	634	0.07	N	Thompson & Townsend 2000
Dempsters Autumn	New Zealand	Oceania	Stream	Aquatic	83	415	0.06	N	Thompson & Townsend 2000
Dempsters Spring	New Zealand	Oceania	Stream	Aquatic	93	538	0.06	N	Thompson & Townsend 2000
Dempsters Summer	New Zealand	Oceania	Stream	Aquatic	107	966	0.08	N	Thompson & Townsend 2000
Stony Stream	New Zealand	Oceania	Stream	Aquatic	112	832	0.07	N	Townsend et al 1998
Canton Creek	New Zealand	Oceania	Stream	Aquatic	108	708	0.06	N	Townsend et al 1998
Black Road Stream	New Zealand	Oceania	Stream	Aquatic	85	373	0.05	N	Townsend et al 1998
Broad Stream	New Zealand	Oceania	Stream	Aquatic	94	565	0.06	N	Townsend et al 1998
Saguaro	US	North America	Desert Giant Cactus Forest	Terrestrial	48	138	0.06	N	Howes 1954
Monterey Bay	US	North America	Marine Intertidal	Aquatic	37	79	0.06	N	Glynn 1965
Pawnee	US	North America	Prairie	Terrestrial	133	416	0.02	N	Harris & Paur 1972
Mojave parasitoids	US	North America	Desert, Chaparral	Terrestrial	37	74	0.05	N	Hawkins & Goeden 1984
Osa scavengers	Costa Rica	Central America	Scavenger Food web on toad carrion in tropical wet lowland	Terrestrial	50	131	0.05	N	Cornaby 1974

Deep Creek	US	North America	Cool desert stream	Aquatic	32	140	0.14	N	Koslucher & Minshall 1973
Aire	UK	Europe	Stream	Aquatic	60	185	0.05	N	Percival & Witehead 1929
Parana	Brazil	South America	River	Aquatic	40	185	0.12	Y, Proportion of diet	Angelini & Agostinho 2005
Itaipu (83-87)	Brazil	South America	Freshwater reservoir	Aquatic	32	139	0.14	Y, Proportion of diet	Angelini et al 2006
Itaipu (88-92)	Brazil	South America	Freshwater reservoir	Aquatic	33	141	0.13	Y, Proportion of diet	Angelini et al 2006
Corrente	Brazil	South America	River	Aquatic	13	34	0.20	Y, Proportion of diet	Angelini et al 2010
Angola	Angola	Africa	Marine	Aquatic	28	127	0.16	Y, Proportion of diet	Angelini & Vaz-Velho 2011
Braco Morto	Brazil	South America	River	Aquatic	39	248	0.16	Y, Proportion of diet	Angelini et al 2013
Onca	Brazil	South America	River	Aquatic	40	241	0.15	Y, Proportion of diet	Angelini et al 2013
Mondego	Portugal	Europe	River Lagoon, Estuarine	Aquatic	26	103	0.15	Y, Proportion of diet	Baeta et al 2011
Vilas	US	North America	Pond	Aquatic	77	958	0.16	N	Schneider 1997
Antarctica	Chile/Argentina/UK claimed region	Antarctica	Marine	Aquatic	28	218	0.28	N	Cornejo-Donoso & Antezana 2008
Huizache	Mexico	North America	Lagoon, Estuarine	Aquatic	26	189	0.28	Y, Proportion of diet	Zetina-Rejon et al 2003
Alvarado	Mexico	North America	Lagoon, Estuarine	Aquatic	30	229	0.25	Y, Proportion of diet	Cruz-Escalona et al 2007
Quick Pond	US	North America	Pond	Aquatic	113	1092	0.09	N	Preston et al 2012
Northern California	US	North America	Marine	Aquatic	80	1448	0.23	Y, Proportion of diet	Ruzicka 2012
Las Cuevas	Belize	Central America	Deciduous Seasonal Forest	Terrestrial	165	114	0.00	N	Lewis et al 2002
Cadiz	Spain	Europe	Marine	Aquatic	44	413	0.21	Y, Proportion of diet	Torres et al 2013
Scotia Sea	Chile/Argentina/UK claimed region	Antarctica	Marine	Aquatic	56	178	0.06	Y, Percent of diet	Hopkins et al 1993
Bear	Norway	Europe/Arctic	Island	Terrestrial	31	43	0.04	N	Hodkinson & Coulson 2004
Wet tropics	Australia	Oceania	River	Aquatic	62	211	0.05	N	Rayner et al 2010

Porteirinho	Brazil	South America	Stream	Aquatic	119	310	0.02	N	Motta & Uieda 2005
Sarracenia	US/Canada	North America	Pitcher Plant	Aquatic	91	1834	0.22	N	Baiser et al 2012

Appendix references

1. Schreiber SJ, Bürger R, Bolnick DI (2011) The community effects of phenotypic and genetic variation within a predator population. *Ecology* 92(8):1582–1593.
2. Vasseur DA, Amarasekare P, Rudolf VHW, Levine JM (2011) Eco-Evolutionary dynamics enable coexistence via neighbor-dependent selection. *Am Nat* 178(5):E96–E109.
3. Gibert JP, Brassil CE (2014) Individual phenotypic variation reduces interaction strengths in a consumer-resource system. *Ecol Evol* 4(18):3703–3713.
4. Gibert JP, DeLong JP (2015) Individual Variation Decreases Interference Competition but Increases Species Persistence. *Adv Ecol Res* 52:45–64.
5. Rall BC, et al. (2012) Universal temperature and body-mass scaling of feeding rates. *Philos Trans R Soc Lond B Biol Sci* 367(1605):2923–34.
6. Brodie Jr. ED, Ridenhour BJ, Brodie III ED (2002) The Evolutionary Response of Predators to Dangerous Prey: Hotspots and Coldspots in the Geographic Mosaic of Coevolution between Garter Snakes and Newts. *Evolution (N Y)* 56(10):2067–2082.
7. Toju H, Sota T (2006) Imbalance of predator and prey armament: geographic clines in phenotypic interface and natural selection. *Am Nat* 167(1):105–117.
8. Williams RJ, Martinez ND (2004) Limits to trophic levels and omnivory in complex food webs: theory and data. *Am Nat* 163(3):458–68.
9. Paine RT (1992) Food-Web analysis through field measurements of per capita interaction strength. *Nature* 355(73–75).
10. Cohen JE, Newman CM (1985) A stochastic theory of community food webs I. Models and aggregated data. *Proc R Soc B Biol Sci* 224:421–448.
11. Martinez ND (1992) Constant connectance in community food webs. *Am Nat* 139(6).
12. Berlow EL, et al. (2004) Interaction strengths in food webs: issues and opportunities. *J Anim Ecol* 73(3):585–598.
13. Dunne JA, Williams RJ, Martinez ND, Wood R a, Erwin DH (2008) Compilation and network analyses of cambrian food webs. *PLoS Biol* 6(4):e102.